

# Monolithic carrier-envelope phase-stabilization scheme

Takao Fuji,\* Jens Rauschenberger,\* Alexander Apolonski,\*\* Vladislav S. Yakovlev, and Gabriel Tempea†

Photonics Institute, Vienna University of Technology, Gusshausstrasse 27/387, A-1040 Vienna, Austria

Thomas Udem, Christoph Gohle, and Theodor W. Hänsch

Max Planck Institute of Quantum Optics, Hans-Kopfermann-Strasse 1, D-85748 Garching, Germany

Walter Lehnert and Michael Scherer

Leybold Optics GmbH, Siemensstrasse 88, D-63755 Alzenau, Germany

Ferenc Krausz‡

Ludwig-Maximilians-Universität and Max Planck Institute of Quantum Optics, D-85478 Garching, Germany

Received August 9, 2004

A new scheme for stabilizing the carrier-envelope (CE) phase of a few-cycle laser pulse train is demonstrated. Self-phase modulation and difference-frequency generation in a single periodically poled lithium niobate crystal that transmits the main laser beam allows CE phase locking directly in the usable output. The monolithic scheme obviates the need for splitting off a fraction of the laser output for CE phase control, coupling into microstructured fiber, and separation and recombination of spectral components. As a consequence, the output yields 6-fs, 800-nm pulses with an unprecedented degree of short- and long-term reproducibility of the electric field waveform. © 2005 Optical Society of America

OCIS codes: 120.5050, 320.7160, 120.3940.

At present, the most widely used technique for stabilizing carrier-envelope (CE) offset frequency ( $f_{\text{CEO}}$ ) is to measure the interference beat signal between the high-frequency and the frequency-doubled low-frequency spectral components of an octave-spanning spectrum and phase lock it to a reference clock.<sup>1-5</sup> This scheme has been termed the  $f$ -to- $2f$  method. It uses a rather complex and alignment-sensitive nonlinear interferometric apparatus and relies on an auxiliary beam split off the main laser output. Hence any phase jitter accumulating between the laser output and the output of the phase control setup appears in the usable laser output even if the electronic phase-locking loop works perfectly. In addition, excessive dispersion of the nonlinear interferometer prevents the broadband output from being compressed to a few-cycle pulse. In this Letter we demonstrate a scheme that allows for CE phase stabilization directly in the usable laser output, resulting in a 70-MHz, 6-fs pulse train with a CE timing jitter of less than 150 as accumulated within 35 min.

When the peak intensity of a pulse and the nonlinearity in a frequency-mixing crystal are large enough, both second-order nonlinear frequency mixing [second-harmonic generation or difference-frequency generation (DFG)] and self-phase modulation (SPM) occur at the same time. In regions of spectral overlap at  $f_{\text{CEO}}$  was observed in thin  $\beta$ -barium borate<sup>6</sup> and zinc oxide<sup>7</sup> crystals; however, demonstration of phase stabilization has not been published so far to the best of our knowledge. In this work we tightly focus few-cycle pulses from a Ti:sapphire oscillator into a highly nonlinear periodically poled magnesium-oxide-doped

lithium niobate (PP-MgO:LN) crystal to induce SPM and DFG<sup>8,9</sup> in the near infrared (see Fig. 1). Owing to the enhanced nonlinear interaction and an improved spatial overlap between the two waves (caused by the absence of walk-off effects), the interferometric beat signal emerging at  $f_{\text{CEO}}$  in the region of spectral overlap is strong enough for reliable CE phase locking.

Further important differences from previous CE phase-locking schemes include the CEO beat signal emerging outside the original laser spectrum (allowing its easy isolation) and moderate dispersion in the nonlinear medium (allowing recompression of the transmitted laser pulses). The implications are numerous and far reaching: (i) Almost the entire laser power is available after CE phase locking for applications such as CE phase-dependent nonlinear processes. (ii) It obviates the need to use a

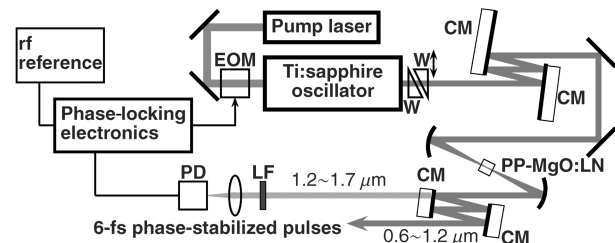


Fig. 1. Experimental realization of the monolithic CE phase-stabilization scheme: Pump laser, frequency-doubled diode-pumped Nd:YVO<sub>4</sub> laser (Coherent Verdi, 532 nm, 3.85 W); W, fused-silica wedged plate; CM, chirped mirror; LF, long-pass filter (cutoff at 1400 nm); PD, InGaAs photodiode; Phase-locking electronics (MenloSystems); rf reference, signal generator (Marconi, 2022D, operated at 1 MHz); EOM, electro-optic modulator.

microstructured fiber, avoiding instabilities associated with coupling into a tiny core. (iii) The full laser power can be used to induce nonlinear processes for locking the CE phase. (iv) The CE phase is controlled directly in the beam that is used for application so that nonlinear amplitude-to-phase conversion is canceled.

The Ti:sapphire oscillator is based on the all-chirped-mirror oscillator described in Ref. 10. It generates pulses with a spectrum extending from 630 to 1015 nm at  $-10$  dB below its maximum. The ultrabroadband chirped mirrors used for intracavity and extracavity dispersion control exhibit tailored dispersion over 620–1100 nm and were manufactured with a Helios magnetron sputtering system by Leybold Optics. The average output power of the oscillator is 220 mW at 3.85 W of pump power and a 70-MHz repetition rate. The spatial profile of the beam is approximately Gaussian. After precompression by a pair of chirped mirrors (compensating for the dispersion of the substrate of the output coupler), the  $\sim 6$ -fs pulses are focused into a 2-mm-long PP-MgO:LN crystal (HC Photonics) with a poling period of 17.7  $\mu\text{m}$ , originally optimized for type 0 ( $e + e \rightarrow e$ ) second-harmonic generation of 1500 nm. The spot size inside the crystal,  $w_0$ , is  $\sim 15$   $\mu\text{m}$ . A chirped mirror acts as a dichroic beam splitter after the crystal. It reflects the fundamental spectrum and transmits the infrared waves at  $>1250$  nm, which emerge from the nonlinear interactions in the PP-MgO:LN crystal. The transmitted beam is passed through a long-pass filter (cutoff of 1400 nm) and is detected by an InGaAs photodiode (New Focus Model 1811-FC).

Figure 2 shows the long-wavelength tail of the spectrum exiting the crystal. Newly generated spectral components in this region are clearly visible when the crystal is translated into the focal region of the laser beam. The main part of the spectrum does not change shape. The infrared light is attributed to SPM and phase-matched DFG. The nonlinear CE phase shift from SPM estimated to  $0.012 \times 2\pi$  rad by numerical simulations is compensated for by the servo system. The beating between the DFG and SPM-generated light at  $f_{\text{CEO}}$  is observed at  $\lambda > 1350$  nm. Optimizing the chirp of the pulses in the crystal by means of wedged fused-silica plates and negative chirped mirrors outside the cavity allows a signal-to-noise ratio of  $>35$  dB in a 100-kHz resolution bandwidth to be achieved, allowing routine CE phase locking with the servo loop system described in Ref. 5. The CEO frequency is clearly visible through a 30% amplitude modulation of the pulse train.

The spatial and temporal matching of the waves interfering in a monolithic device is expected to improve the CE phase control over conventional schemes. To demonstrate this, the laser beam that emerges from our setup in Fig. 1 is focused into another PP-MgO:LN crystal for a second independent CE phase measurement. To our knowledge, such an out-of-loop characterization of CE phase stabilization without fiber broadening<sup>11–14</sup> has not been performed so far. The beat is filtered and amplified just as in the locking loop. We detect low-frequency drifts in the CE phase

by recording the phase error between the reference signal at 1 MHz and the out-of-loop beat signal with a vector voltmeter (HP8405A). For observation of the high-frequency jitter the signal is also monitored by a fast digital oscilloscope. The oscilloscope and the reference frequency generator are referenced to a high-quality quartz clock for better measurement stability. The two-sided power spectrum of phase fluctuations  $S_\phi(\nu)d\nu$ , which is the absolute square of the Fourier transform of CE phase  $\phi(t)$ , as derived from the recorded time series, is shown in Fig. 3. The lowest resolved frequency component is given by the observation time of 35 min. Since the CE phase advance is measurable only when a pulse arrives, the pulse train samples the  $f_{\text{CEO}}$  signal, and the highest possible Fourier frequency describing the jitter of the CE phase becomes one half of  $f_r$  (Nyquist theorem). The phase error integrated from  $f_r/2 = 35$  MHz to 0.48 mHz is  $0.047 \times 2\pi$  rad, or 133 as, of timing jitter at the center wavelength of  $\sim 840$  nm.

Figure 3 reveals an improvement in the accumulated phase error as compared with the most comprehensive out-of-loop CE phase jitter measurement on a conventional system reported in Ref. 15. The most significant difference appears in the low-frequency region ( $<10$  mHz) in which amplitude-to-phase coupling in microstructured fiber is dominant. A large phase error step ( $\sim 0.1 \times 2\pi$  rad, or 270 as) in Ref. 15 is much less pronounced in our results. With the same integration time (from 102.4 kHz to 0.9765 mHz) used in

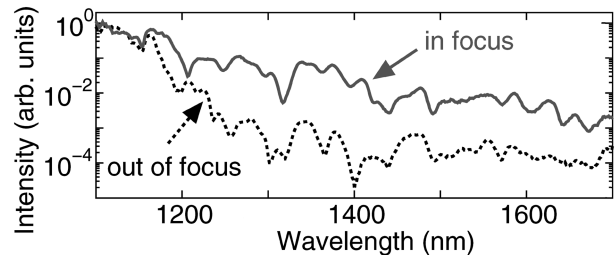


Fig. 2. Long-wavelength tail of the laser spectrum exiting the nonlinear crystal, measured with an optical spectrum analyzer (Ando AQ-6315A). The solid curve shows the optimized spectrum, whereas the dotted curve depicts it with the crystal shifted out of focus, for reference.

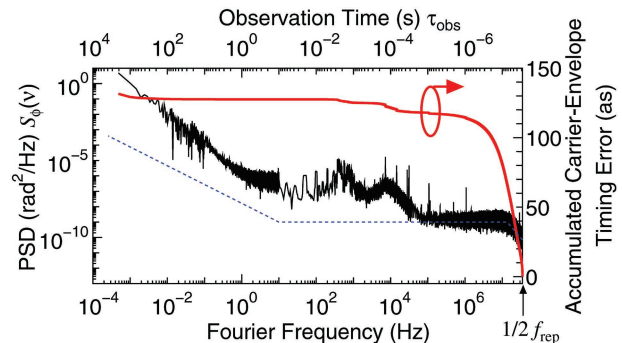


Fig. 3. Out-of-loop two-sided phase-noise power spectral density (PSD) and integrated CE timing error calculated from  $\Delta\phi_{\text{rms}} = [2 \int_{-f_r/2}^{-1/\tau_{\text{obs}}} S_\phi(\nu)d\nu]^{1/2}$ . The dotted curve shows the noise floor of the photodetector and the vector voltmeter for low frequencies.

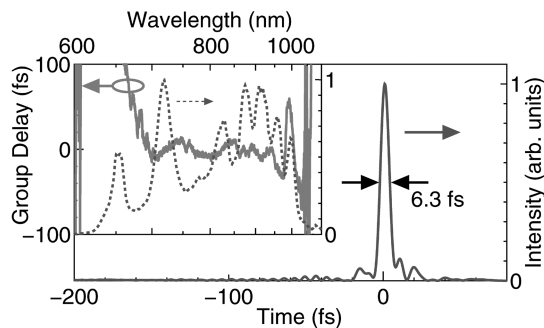


Fig. 4. Temporal profile of the output pulses of the phase-stabilized system (passing through the 2-mm length of PP-MgO:LN and compressed with chirped mirrors) as retrieved from a SPIDER measurement. The FWHM of the intensity profile is 6.3 fs. Inset, group delay (solid curve) and spectrum (dotted curve, linear scale) of the pulses.

Ref. 15, our integrated phase error is  $0.022 \times 2\pi$  rad, corresponding to 62 as of timing jitter, which is a five-fold improvement. For frequencies above 100 kHz the CE phase noise is actually lower than our current noise floor set by the photodetector. Nevertheless we can use the recorded noise in this frequency region as an upper limit.

In the present system the mirror compressor and the crystal have a combined loss of  $\sim 30\%$  (owing to the mirror coating quality, the photorefractive effect in the crystal, etc.); nevertheless this is much more efficient than the conventional  $f$ -to- $2f$  scheme. The dispersion of the crystal can be compensated for by chirped mirrors.

The pulse energy passed through the compressor is 160 mW,  $\sim 2.3$  nJ. The compressed pulses are characterized with broadband spectral phase interferometry for direct electric field reconstruction (SPIDER),<sup>16</sup> and the results are summarized in Fig. 4. We verified the absence of serious phase distortions from nonlinear frequency mixing by comparing the SPIDER results with the crystal being in focus and out of focus. The measurements yielded a pulse width of 6.3 fs, whereas the transform-limited pulse width is 4.1 fs, in both cases. The remaining spectral phase imperfection could in principle be compensated for by an appropriately designed compressor.

In conclusion, we have demonstrated a simple, highly efficient monolithic scheme for direct CE phase stabilization of a mode-locked laser delivering few-cycle pulses. In the first implementation of the new concept, CE phase-locked, 6.3-fs pulses with several nanojoules of pulse energy were produced at a repetition rate of 70 MHz with unprecedented long-term reproducibility of the generated few-cycle waveforms. The scheme can be adapted to lasers operating in other wavelength regions. The demonstrated technology may be a key to pushing the frontier of attosecond science to the atomic time scale ( $<100$  as).

We gratefully acknowledge support from the FWF (Austria) through grants Z63 and P15382. T. Fuji

(tkf@mpq.mpg.de) acknowledges support from the Japan Society for the Promotion of Science Postdoctoral Fellowships for Research Abroad.

*Note added in proof:* After improving the system (output power of the oscillator, period of the crystal, and compressor mirrors), the CEO beat emerges with a 55-dB signal-to-noise ratio (resolution bandwidth 100 kHz), resulting in a further reduction of the CE-phase jitter to 43 as (0.2 MHz–35 MHz).

\*Present address, Max Planck Institute of Quantum Optics, Hans-Kopfermann-Strasse 1, D-85748 Garching, Germany.

\*\*Also with the Institute of Automation and Electrometry, Russian Academy of Science, Novosibirsk, Russia.

†Also with Femtolasers Produktions GmbH, Fernkogasse 10, A-1100 Vienna, Austria.

‡Also with the Photonics Institute, Vienna University of Technology, Gusshausstrasse 27/387, A-7040 Vienna, Austria.

## References

1. J. Reichert, R. Holzwarth, T. Udem, and T. W. Hänsch, *Opt. Commun.* **172**, 59 (1999).
2. H. R. Telle, G. Steinmeyer, A. E. Dunlop, J. Stenger, D. H. Sutter, and U. Keller, *Appl. Phys. B* **69**, 327 (1999).
3. D. J. Jones, S. A. Diddams, J. K. Ranka, A. Stentz, R. S. Windeler, J. L. Hall, and S. T. Cundiff, *Science* **288**, 635 (2000).
4. R. Holzwarth, T. Udem, T. W. Hänsch, J. C. Knight, W. J. Wadsworth, and P. St. J. Russell, *Phys. Rev. Lett.* **85**, 2264 (2000).
5. A. Poppe, R. Holzwarth, A. Apolonski, G. Tempea, C. Spielmann, T. W. Hänsch, and F. Krausz, *Appl. Phys. B* **72**, 373 (2001).
6. A. Apolonski, A. Poppe, G. Tempea, C. Spielmann, T. Udem, R. Holzwarth, T. W. Hänsch, and F. Krausz, *Phys. Rev. Lett.* **85**, 740 (2000).
7. O. D. Mücke, T. Tritschler, M. Wegener, U. Morgner, and F. X. Kärtner, *Opt. Lett.* **27**, 2127 (2002).
8. M. Zimmermann, C. Gohle, R. Holzwarth, T. Udem, and T. W. Hänsch, *Opt. Lett.* **29**, 310 (2004).
9. T. Fuji, A. Apolonski, and F. Krausz, *Opt. Lett.* **29**, 632 (2004).
10. T. Fuji, A. Unterhuber, V. S. Yakovlev, G. Tempea, A. Stingl, F. Krausz, and W. Drexler, *Appl. Phys. B* **77**, 125 (2003).
11. U. Morgner, R. Ell, G. Metzler, T. R. Schibli, F. X. Kärtner, J. G. Fujimoto, H. A. Haus, and E. P. Ippen, *Phys. Rev. Lett.* **86**, 5462 (2001).
12. T. M. Ramond, S. A. Diddams, L. Hollberg, and A. Bartels, *Opt. Lett.* **27**, 1842 (2002).
13. T. M. Fortier, D. J. Jones, and S. T. Cundiff, *Opt. Lett.* **28**, 2198 (2003).
14. L. Matos, O. Kuzucu, T. Schibli, J. Kim, E. Ippen, D. Kleppner, and F. Kärtner, *Opt. Lett.* **29**, 1683 (2004).
15. T. M. Fortier, D. J. Jones, J. Ye, and S. T. Cundiff, *IEEE J. Sel. Top. Quantum Electron.* **9**, 1002 (2003).
16. C. Iaconis and I. A. Walmsley, *IEEE J. Quantum Electron.* **35**, 501 (1999).